Advances in Natural Fiber Cement Composites: A Material for the Sustainable Construction Industry*

Flávio de Andrade Silva[1], Barzin Mobasher[2], Romildo Dias de Toledo Filho[3]

Summary: The need for economical, sustainable, safe, and secure shelter is an inherent global problem and numerous challenges remain in order to produce environmentally friendly construction products which are structurally safe and durable. The use of sisal, a natural fiber with enhanced mechanical performance, as reinforcement in a cement based matrix has shown to be a promising opportunity. This work addresses the development and advances of strain hardening cement composites using sisal fiber as reinforcement. Sisal fibers were used as a fabric to reinforce a multi-layer cementitious composite with a low content of Portland cement. Monotonic direct tensile tests were performed in the composites. The crack spacing during tension was measured by image analysis and correlated to strain. Local and global deformation was addressed. To demonstrate the high performance of the developed composite in long term applications, its resistance to tensile fatigue cycles was investigated. The composites were subjected to tensile fatigue load with maximum stresses ranging from 4 to 9.6 MPa at a frequency of 2 Hz. The composites did not fatigue below a maximum fatigue level of 6 MPa up to 10^6 cycles. Monotonic tensile testing was performed for composites that survived 10^6 cycles to determine its residual strength.

1 Introduction

Academic institutions and fiber cement producers have been engaged for the past 25 years in intensive research to find substitutes and to develop processes for the industrial production of asbestos free fiber materials. Some products are already produced on a commercial basis using cellulose pulp [1] and fibrillated polypropylene networks-glass fibers as reinforcement [2]. Polyvinyl alcohol (PVA) fibers and a combination of cellulose and short PVA fibers have also been proposed for asbestos replacement [3]. A considerable effort has also been

* This is a peer-reviewed paper. Online available: urn:nbn:de:bsz:14-ds-1244048177249-62278
[1] Visiting Researcher D.Sc., Institute of Construction Materials, TU Dresden
[2] Prof. Ph.D., Department of Civil and Environmental Engineering, Arizona State University (ASU)
[3] Prof. D.Sc., Department of Civil Engineering, Universidade Federal do Rio de Janeiro (UFRJ)

directed toward the application of vegetable fibers such as sisal and coconut to replace asbestos fibers because of their availability in the tropical and subtropical parts of the world, low cost and low consumption of energy [4-9].

Vegetable fibers such as sisal, jute and coconut have been used as reinforcement of cementitious matrices in the form of short filament fibers [9,10]. Short filament geometry composites presented a tension softening behavior with low tensile strength, resulting in products which are more suitable for non-structural applications. Pulp fibers derived from wood, bamboo and sisal have also been used as reinforcement [11-15]. The later composites presents two major drawbacks: i) the process for pulp dispersion in water is very time and energy consuming ii) the matrix is a cement paste which presents high consume of cement, hence, elevated emission of CO_2 to the atmosphere and high shrinkage. Such composites are being proposed to be used in non-structural applications and also presented a tension softening behavior. In order to produce a composite reinforced with natural fibers that present tension hardening behavior, long sisal fibers were employed and a textile composite was developed in the present study. Such family of composites is defined as textile reinforced concrete (TRC). The TRC allows the design of thin walled elements with high strength in tension and compression. These composites can be used in various fields of applications such as permanent formworks, facades, tanks, pipes, long span roofing elements, strengthening of existing structures and structural building members.

Vegetable fiber cement composites produced with ordinary Portland cement matrices undergo an aging process in humid environments in which they may suffer a reduction in post-cracking strength and toughness. This durability problem is associated with an increase in fiber fracture and decrease in fiber pull-out due to fiber mineralization. This mineralization process is a result of migration of hydration products (mainly $CaOH_2$) to the fiber structure. Efforts to develop durable cement composite laminates reinforced by long sisal fibers for structural purposes has shown much promise recently [16,17]. A newly developed matrix with a low Calcium Hydroxide content was used. This matrix increases the long term durability of the natural fiber with a low cement content (only 50% as compared to conventional systems) that helps reduce CO_2 emissions and cost, resulting in a sustainable alternative. In the present research a modified matrix that was previously investigated and showed no strength and toughness reduction after accelerated aging was used.

This work presents recent advances on the mechanical behavior of durable sisal fiber reinforced cement composites. Monotonic direct tensile tests were performed in the composites. The crack spacing during tension was measured by image analysis and correlated to strain. Local and global deformation was addressed. To demonstrate the high performance of the developed composite in long term applications, its resistance to tensile fatigue cycles was investigated. The composites were subjected to tensile fatigue load with maximum stresses ranging from 4 to 9.6 MPa at a frequency of 2 Hz. These stress levels represents approximately 30% and 80% of the UTS, respectively. The fatigue tests were stopped either at 10^6

cycles or complete failure of the composite, whichever occurred first. Composites that survived 10^6 cycles were tested under monotonic tension to establish its residual strength.

2 Experimental Program

2.1 Sisal Fiber

The sisal fibers used in this investigation were characterized by Silva et al. and they presented a mean density, elastic modulus and tensile strength of 0.9 g/cm^3, 19 GPa and 400 MPa, respectively [18]. These fibers were extracted from the sisal plant in a farm located in the city of Valente, state of Bahia – Brazil. They present an irregular cross section (see Fig. 1) with mean area ranging from 0.04 to 0.05 mm^2. The sisal plant leaf is a functionally graded composite structure which is reinforced by three types of fibers: structural, arch and xylem fibers. The first occurs in the periphery of the leaf providing resistance to tensile loads. The others present secondary reinforcement, occurring in the middle of the leaf, as well as, a path for nutrients. Sisal fibers contain numerous fiber-cells which are about 6 to 30 μm in diameter [19]. The individual fiber-cells are linked together by means of the middle lamella, which consist of hemicellulose and lignin. Each individual fiber-cell is made up of four main parts, namely the primary wall, the thick secondary wall, the tertiary wall and the lumen.

After receiving the sisal fibers they were washed and cutted to the size of the molds (400 mm). The fibers were weighted and separated so it could be added to the matrix in five different layers resulting in a total volume fraction of 10% (see section 2.3). The sisal fibers were stitched by three cotton fibers to make the spacing between the fibers more homogeneous therefore facilitating the molding process.

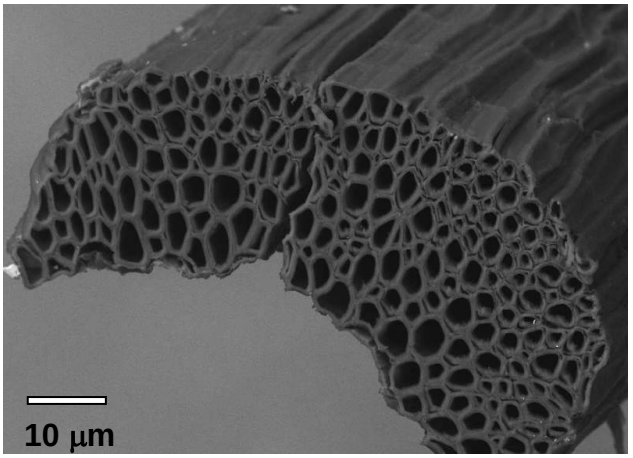

Fig. 1: The sisal fiber micro-structure.

2.2 Matrix Modifications

The matrix was produced using the Portland cement CPII F-32 defined by the Brazilian standard [20] as composed with filler (in mass: 85% < clinker < 91%; 3% < gypsum < 5%; 6% < filler < 10%) with a 28 days compressive strength of 32 MPa. Following the recommendations of previous studies, in order to increase the durability of the composites, the Portland cement was replaced by 30% of MK and 20% of CWCCB [16,17]. The metakaolin (MK) was obtained from Metacaulim do Brasil Industria e Comércio LTDA, and calcined waste crushed clay brick (CWCCB) from an industry located in Itaborai – RJ, Brazil, calcined at 850 ^{o}C. The mortar matrix used in this study presented a mix design 1 : 1 : 0.4 (cementitious material : sand : water by weight). The used river sand presented a maximum diameter of 1.18 mm and density of 2.67g/cm^3. A naphthalene superplasticizer Fosroc Reax Conplast SP 430 with content of solids of 44% was used to increase the fluidity of the matrix.

Wollastonite fibers (JG class), obtained from Energyarc, were used as a micro-reinforcement in the composite production. Wollastonite JG class ($CaSiO_3$) is a naturally occurring white, non-metallic mineral with an acicular morphology. It presents an average equivalent diameter of 40 μm with an aspect ratio of 15.

2.3 Composite Manufacturing

The matrix was produced using a bench-mounted mechanical mixer of 20 liters capacity. The cementitious materials were homogenized by dry mixing for 30 seconds prior to addition of sand and 5% by volume of wollastonite. The powder material was mixed for and additional 30 seconds prior to addition of superplasticizer and water. The mixture was blended for 3 minutes. For the production of the laminates, the mortar mix was placed in a steel mold, one layer at a time, followed by single layers of long unidirectional aligned fibers (up to 5 layers). The samples were consolidated using a vibrating table operated at a frequency of 65 Hz, resulting in a sisal fiber volume fraction of 10%. After casting the composites were compressed at 3 MPa for 5 minutes. The compression load was applied in the face that the matrix was placed. The specimens were covered in their molds for 24 hours prior to moist curing for 28 days in a cure chamber with 100% RH and 23 ± 1 ^{0}C.

2.4 Testing

Direct tensile tests were performed in an Instron universal testing machine with a capacity of 500 kN. The tests were controlled by the cross-head displacement at a rate of 0.1 mm/min. Six specimens measuring 400 mm x 50 mm x 12 mm (length x width x thickness) were tested using a gage length of 300 mm with fixed–fixed boundary conditions. Aluminum thin sheets

were glued on both ends of the specimen and the pressure of the hydraulic grips was adjusted to 1.37 MPa (200 psi) in order to minimize stress concentration and damage. The tensile load, cross head displacement and strain were recorded. The tensile strains were also measured by a strain gage glued on the center of the specimen, and also the stroke displacement. The crack spacing during tension was measured by image analysis and correlated to strain. For more information on crack spacing measurements see elsewhere [21].

The composites were tested under tensile fatigue loading at a stress ratio (R ratio = $\sigma_{min}/\sigma_{max}$) of 0.2 and frequency of 2 Hz. Testing was conducted on a MTS 810 testing system under force control. The experiment was conducted in samples with a 300 mm gage length at five different stress levels: 4, 4.8, 6, 7.2, and 9.6 MPa. Three samples were tested for each stress level and they presented exactly the same geometry (400 mm x 50 mm x 12 mm – length x width x thickness) as the ones used in the monotonic tests. The tests were stopped after 10^6 cycles or after failure, whichever occurred first. Specimens that survived 10^6 cycles were tested under monotonic tensile load using the same testing system (MTS 810).

3 Discussion and Results

Fig. 2 shows a typical tensile stress strain response of the sisal fiber reinforced composite system. Two measures of tensile strain are used including the localized strain measured from the electrical resistance gage and the nominal strain defined by dividing the cross head stroke displacement by the specimen length. These responses differ at various stages of loading since they furthermore correspond to stages of crack initiation, propagation, distribution, opening, and localization. Five distinct zones are identified using roman numerals with two zones prior to and three zones after the bend over point (BOP). Fig. 2b shows both the initial response and also the overall response of the stress strain curve using a multi-scale axis representation. Note that the measurements of these two gages allow differentiation of the response ranges. Zone I corresponds to the elastic-linear range where both matrix and the fiber behave linearly. Due to low volume fraction of fibers (≤ 10%) the stiffness of the composite is dominated by matrix properties and this zone is limited to strain measures of up to 150 - 175 μstr. The initial stress-strain response is marked by a limited range of linear elastic portion as the two strain measures are almost the same, and the specimen exhibits the highest stiffness. The linear zone is terminated by initial crack formation in the matrix phase (reported as of σ_{BOP}- from experiments) as shown in Fig. 2a. After the initiation of cracks in the matrix, its load carrying capacity does not vanish as the cracks are bridged by the longitudinal fibers.

Immediately after the initiation of first matrix crack, other matrix cracks also initiate throughout the specimen at approximately regular intervals and begin to propagate across the width. The strain recorded by the resistance gage remains relatively constant in this range which indicates a steady state condition of several cracks that initiate and propagate across

the width of the specimen. The strain range within Zone II is associated with formation of matrix cracks, however, no single crack has traversed the entire width. The term defined as BOP+ corresponds to the stress level at which the first matrix crack completely propagates across the width. As indicated in the experimental results shown in Fig. 5a and 5b the linear behavior terminates at the σ_{BOP-} = 3.63-4.86 MPa. The bend over point ranges from the beginning of non-linearity at 4.80 MPa to a point where the slope drastically decreases (σ_{BOP+} = 4.80 - 5.59 MPa). Zone II is therefore defined as the stable cracking range between the two stress levels of σ_{BOP-} and σ_{BOP+}.

The post BOP stage is characterized by formation of distributed cracking in Zone III. In this homogenization phase, as the applied strain increases, more cracks form and the spacing decreases in an exponential manner. The strain measured by the strain gage remains constant while several cracks form throughout the section as shown in Fig. 2b.

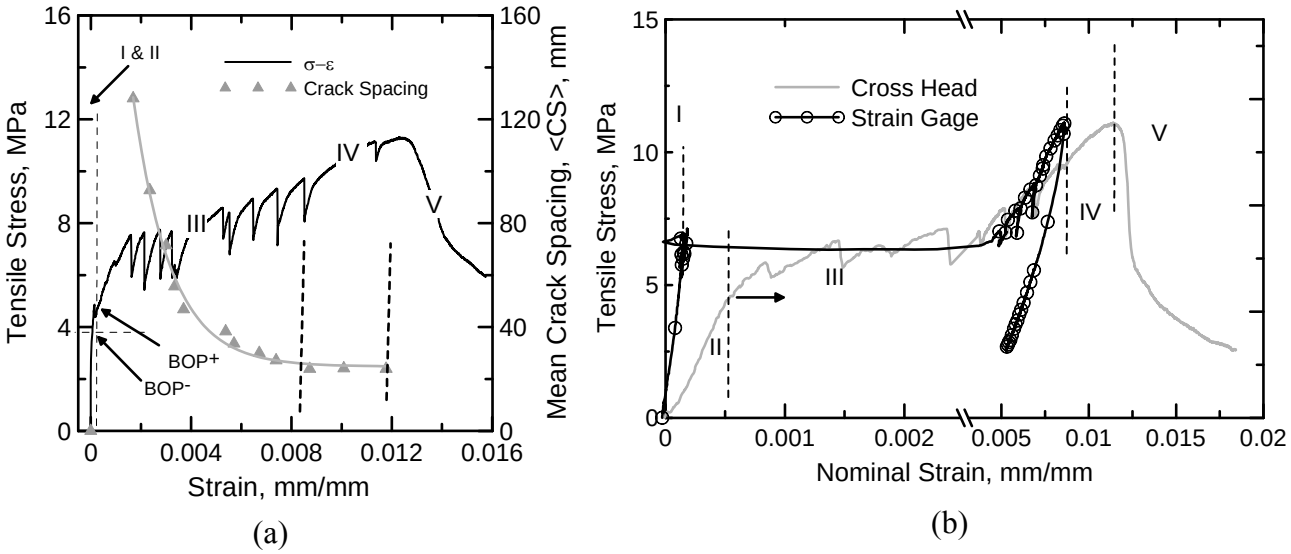

Fig. 2: Tensile response of the sisal fiber reinforced composite system.

The crack spacing measurements as shown in Fig. 2a show a general reduction in spacing during loading until a steady state condition is reached. This zone covers a range at the end of Zone II and remain constant throughout Zone IV. This constant level of crack spacing is defined as saturation crack spacing. Beyond this point, reduction in crack spacing is not observed since no new cracks are forming, and additional imposed strain results in widening of the existing cracks as verified by the pictures of the specimen under the load.

It can be seen from Fig. 2a that at a strain of 0.0016 mm/mm (Zone III) the cracking spacing drastically decreases from an initial value of 130 mm to 45 mm. During the multiple crack

formation the crack spacing decreases until a point (beginning of Zone IV) where it becomes constant at 23 mm.

Zone IV corresponds to the completion of cracking phase and initiation of debonding. Note that the strain gage recording fails to increase as the same rate of the overall strain measure and no additional cracks are formed. As the cracking saturates in the specimen, Zone IV is dominated by progressive damage and characterized by a crack widening stage ultimately leading to failure by fiber pullout. The average ultimate strain of the composite is 1.53 % (measured from cross-head displacement) which shows the capacity of the sisal fibers to cause crack distribution. The average ultimate strength of 12 MPa and an initial modulus of 34.17 GPa is indicative that sisal fiber reinforced cement composite presents a mechanical performance high enough for structural level applications.

Fig. 3 shows the stress versus cycles behavior of the sisal reinforced cement composite tested at various maximum tensile stresses (4 MPa - 9.8 MPa). It can be seen that the composites can survive 10^6 cycles up to 6 MPa, which represents 50% of its UTS. The stress level of 6 MPa can be considered a threshold limit where composites may present fatigue failure at cycles close to 10^6.

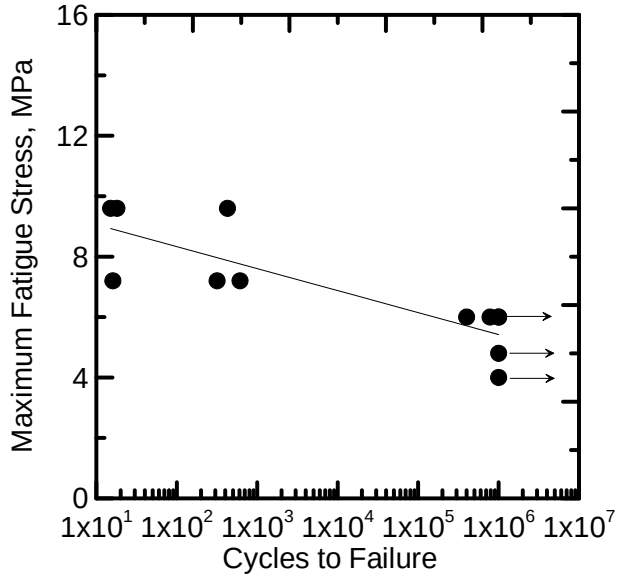

Fig. 3: Stress versus cycles fatigue curve for composites subjected various fatigue stress levels.

Beyond 6 MPa all the composites failed below reaching 10^3 cycles. It was observed that for high stress levels (i.e. > 6 MPa) all the cracks are formed at the first cycles. The number of cracks (12) were the same as the ones observed in monotonic tensile tests. After the crack formation cracks started to widen. The cycles at these high stress levels caused a degradation process in the fiber-matrix interface which increased the rate of cracking opening leading the composite to complete failure at low cycles (i.e. < 10^3).

Composites that survived 10^6 cycles were tested under monotonic tensile load and the results are presented in Fig. 4. When comparing the UTS from monotonic to post-fatigue tensile tests a slight decrease was observed. Nevertheless, this decrease lies in the standard variation range of the monotonic tests and no significant variation among the post-fatigue UTS for different stress levels was observed. Stiffness degradation was observed when calculating the modulus for the post-fatigue tensile tests. Fig. 4b shows that samples subjected to a maximum fatigue stress level of 4 MPa presented modulus in the same range as the one calculated for the monotonic tensile tests. Above 4 MPa the modulus started to decrease from approximately 11.5 to 2 GPa. It is important to mention that these modulus were calculated from cross-head displacement data. First crack strength was also computed for post-fatigue tensile tests. The composites presented increased first crack strength for higher maximum fatigue stress levels (see Fig. 4 b). These evidences may indicate that the matrix is becoming stiffer after 10^6 cycles when increasing the fatigue stress levels but the interfacial transition zone is degrading.

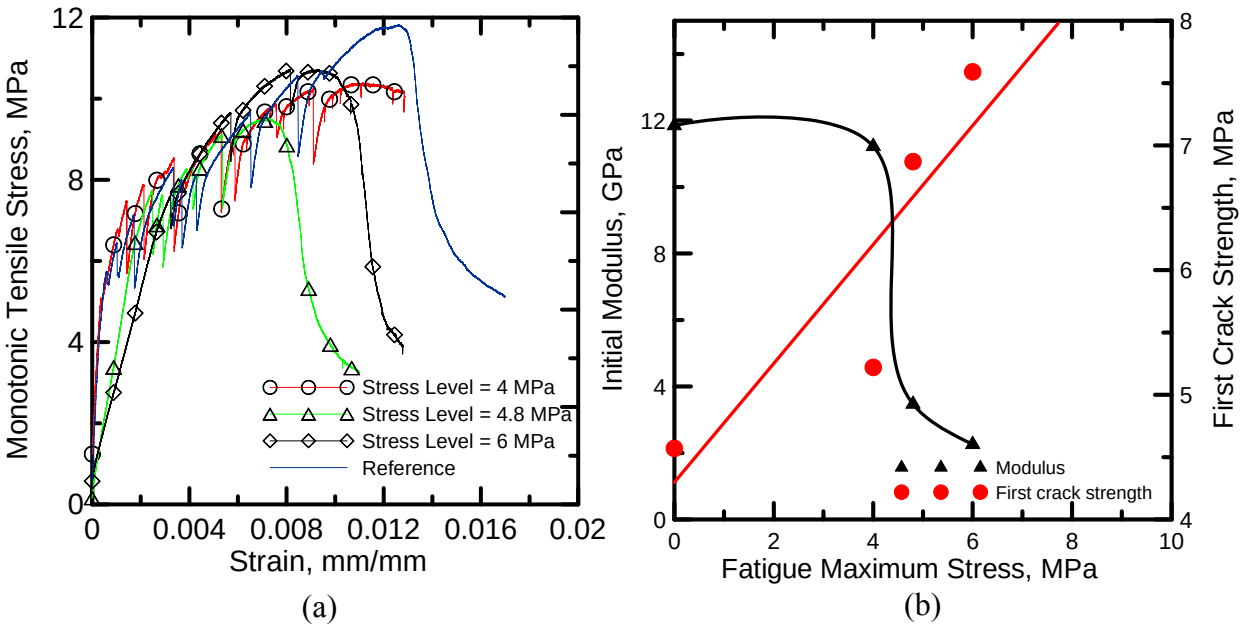

Fig. 4: Monotonic tensile behavior of composites that have survived 10^6 cycles.

To understand the evolution of damage, stress-strain hysteresis measurements were conducted at various stress levels. These are shown in Fig. 5. These plots were obtained from composites that survived 10^6 cycles at maximum stress levels of 4, 4.8 and 6 MPa. The Young's modulus was computed from the unloading portion of the cycle for several cycles. For the maximum stress level of 4 MPa the thickness of the individual hysteresis loops, a measure of inelastic damage or energy during a given cycle, was not significant and did not change with cycles. No stiffness degradation was observed for this stress level. When increasing the ma-

ximum fatigue stress to 4.8 and 6 MPa a different behavior was observed. An increase in the thickness of the hysteresis loops as a function of cycles was observed for both levels. This behavior can be explained due to the formation of several cracks in the first cycles and posterior widening of these cracks. Higher degradation was observed for the composites cycled at a maximum stress of 6 MPa. At 10^6 cycles the maximum strain was 0.8 % and Young´s modulus of 4.2 GPa. For the 4.8 MPa stress level the maximum strain was 0.23% and Young´s modulus of 2 GPa was computed at 10^6 cycles.

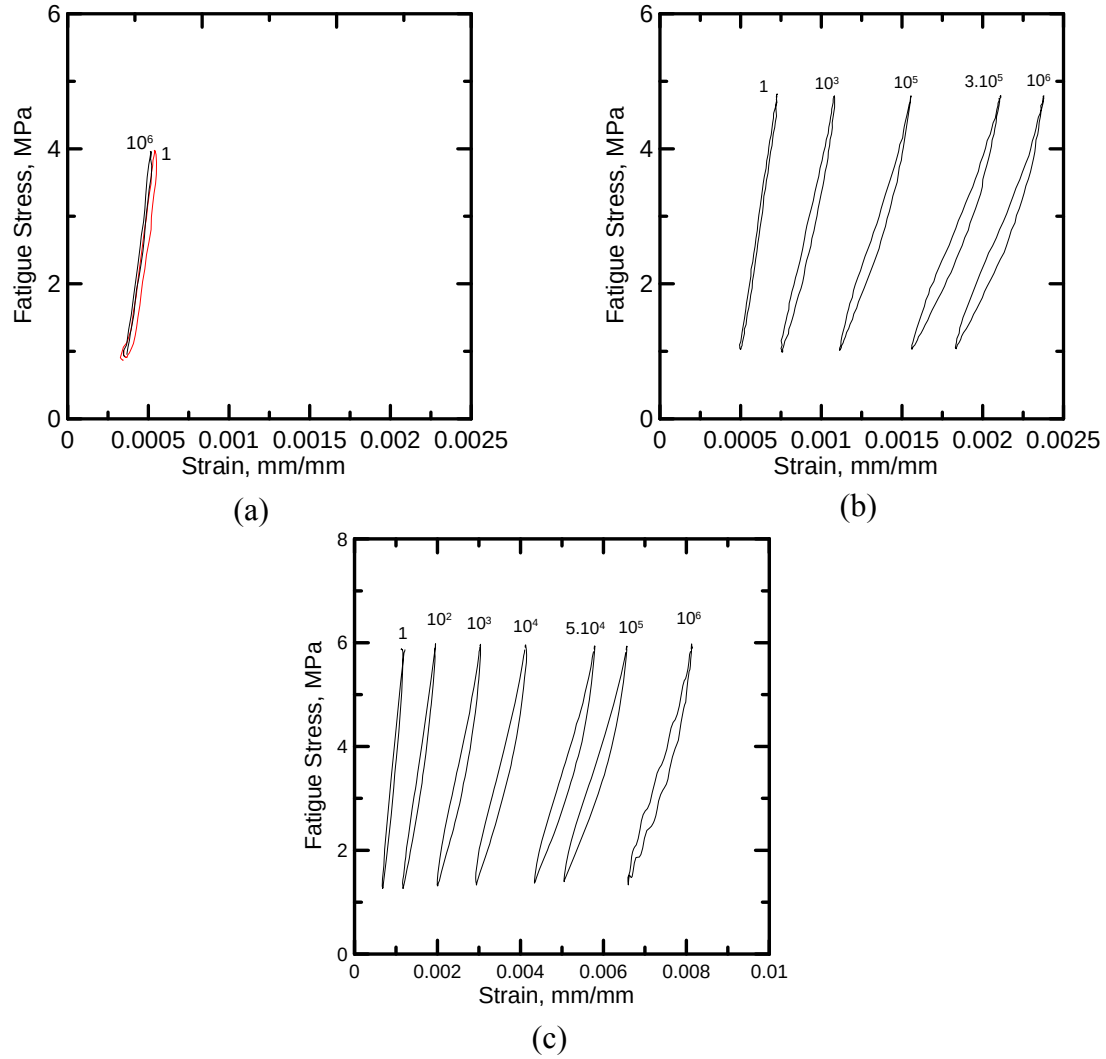

Fig. 5: Hysteresis stress-strain behavior of composites subjected to 10^6 cycles.

Samples that were tested under fatigue up to 10^6 cycles and did not failed were pre-loaded to 0.4% strain and then glued with epoxy so the cracks remained open. These samples were then embedded in a highly fluid polymer in order to be analyzed using the an optical microscope. Fig. 6 shows the capacity of the fibers to arrest and bridge the cracks formed during fatigue cycles in lateral cross section views. This behavior attests the high efficiency in the fiber mat-

rix bond adhesion of the composite system even when subjected to 10^6 cycles at a maximum stress of 6 MPa.

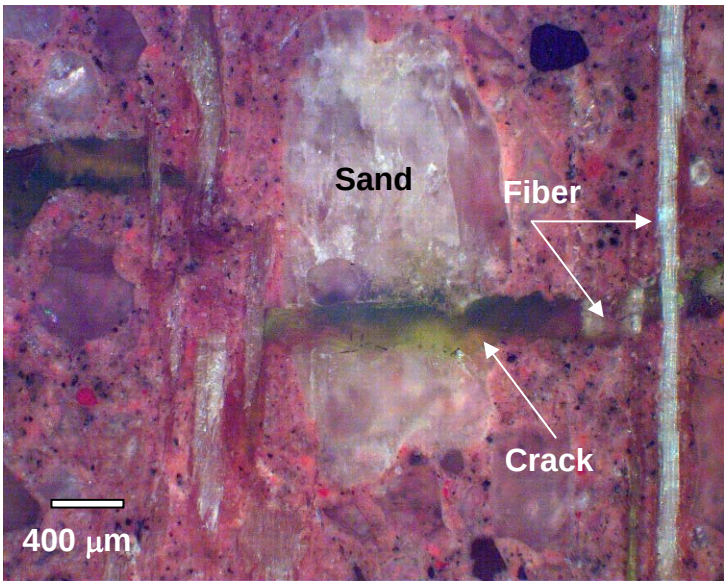

Fig. 6: Fibers bridging the cracks on composites subjected to 10^6 cycles.

4 Conclusions

Use of continuous sisal fabrics that are formed by aligning and stitching the fibers in a multi-layer cement composite system present a new perspective for the use of natural fiber reinforced composites in the construction industry. A matrix with a low content of Portland cement and calcium hydroxide was used to reduce the potential aging of sisal fibers.

The composites showed high modulus at linear-elastic zones ranges with elastic moduli around 34 GPa under direct tension. Multiple cracking behavior was observed under tensile loads with average UTS of 12 MPa at a strain of approximately 1.50 %.

Composites did not fatigue up to 10^6 cycles when subject to maximum stress level below 6 MPa. Above this stress the composites presented fatigue below 10^3 cycles. Composites that survived 10^6 cycles and were tested under monotonic tension did not present significant reduction in UTS but presented decrease in Young´s modulus. The first crack strength increased when increasing the fatigue stress levels. From the hysteresis stress-strain curves it was noticed no signs of degradation for maximum stress level of 4 MPa. For maximum stress levels of 4.8 and 6 MPa there was noticed an increase in the hysteresis area and decrease in the Young´s modulus.

5 References

[1] COUTTS, R.S.P. Wood fibre reinforced cement composites, IN: SWAMY, R.N. (EDITOR) *Natural Fibre Reinforced Cement and Concrete*, VOL. 5, BLACKIE AND SON LTD., *London,* 1988, PP.1-62.

[2] XU, G.; MAGNANI, S., MESTURINI, G.; HANNANT, D.J.: Hybrid polypropylene-glass/cement corrugated sheets. *Composites: Part A* 27 (1996), p. 459-466.

[3] HIKASA, J.; GENBA, T.; MIZOBE, A.; OKAZAKI, M. Replacement for asbestos in reinforced cement products – "Kuralon" PVA fibers, properties, structure. In: *International Man-Made Fibers Congress*, Dornbirm, 1986.

[4] GRAM, H.-E. Durability of natural fibers in concrete. *Swedish Cement and Concrete Research Institute*, Research FO. 1:83, STOCKHOLM, 1983.

[5] BERHANE, Z.: Performance of natural fiber reinforced mortar roofing tiles. *Materials and Structures* 27 (1999), P. 347-352.

[6] CANOVAS, M.F.; SELVA, N.H.; KAWICHE, G.M.: New economical solutions for improvement of durability of portland cement mortars reinforced with sisal fibers. *Materials and Structures* 25 (1992), P. 417-422.

[7] TOLEDO FILHO, R.D.: *Natural fiber reinforced mortar composites: experimental characterisation*, Department of Civil Engineering- Pontifical Catholic University of Rio de Janeiro-(PUC-Rio), 1997 – Ph.D. thesis.

[8] TOLEDO FILHO, R. D.; JOSEPH, K.; GHAVAMI, K.; ENGLAND, G.L.: The use of sisal fiber as reinforcement in cement based composites. *Brazilian Journal of Agricultural and Environmental Engineering* 3 (1999), P. 245-256.

[9] TOLEDO FILHO, R.D.; SCRIVENER, K.; ENGLAND, G.L; GHAVAMI, K.: Durability of alkali-sensivite sisal and coconut fibers in cement mortar composites. *Cement and concrete composites* 22 (2000), P. 127-143.

[10] RAMAKRISHNA, G.; SUNDARARAJAN, T.: Impact strength of a few natural fibre reinforced cement mortar slabs: a comparative study. *Cement and Concrete Composites* 27 (2005), P. 547-553.

[11] SILVA, F.A.; GHAVAMI, K.; D'ALMEIDA, J.R.M. Bamboo-Wollastonite Hybrid Cementitious Composites: Toughness Evaluation. In: *Joint ASME/ASCE/SES Conference on Mechanics and Materials*, *Baton Rouge* , 2005.

[12] SILVA, F.A.; GHAVAMI, K.; D'ALMEIDA, J.R.M.. Toughness of cementitious composites reinforced by randomly distributed sisal pulps. *In: Eleventh International Conference on Composites/Nano Engineering (icce - 11), Hilton-Head Island, 2004.*

[13] SILVA, F.A.; GHAVAMI, K.,; D'ALMEIDA,: J.R.M. Behavior of CRBP-AL subjected to impact and static loading. *In: 17th ASCE Engineering Mechanics Conference (EM 2004), Delaware*, 2004.

[14] MOHR, B.J.; NANKO, H.; KURTIS, K.E.: Durability of Kraft Pulp Fiber-Cement Composites to Wet/Dry Cycling. *Cement and Concrete Composites* 27 *(* 2005), P. 435-448.

[15] ROMA JR., L.C.; MARTELLO, L.C.; SAVASTANO JR, H.: Evaluation of mechanical, physical and thermal performance of cement-based tiles reinforced with vegetable fibers. *Construction & Building Materials* 22 (2008), P. 668-674.

[16] SILVA, F.A.; MELO FILHO, J.A.; TOLEDO FILHO, R.D.; FAIRBAIRN E.M.R. Mechanical behavior and durability of compression moulded sisal fiber cement mortar laminates (SFCML). *In: 1st International RILEM Conference on Textile Reinforced Concrete (ICTRC)*, *Aachen*, 2006, pp. 171-180.

[17] TOLEDO FILHO, R.D.; SILVA, F.A.; FAIRBAIRN, E.M.R.; MELO FILHO, J.A.: Durability of compression molded sisal fiber reinforced mortar laminates. *Construction and Building Materials* 23 (2009), P. 2409-2420.

[18] SILVA, F.A.; CHAWLA, N.; TOLEDO FILHO, R.D. Tensile behavior of high performance natural (sisal) fibers. *Composites Science and Technology* 68 (2008), P. 3438-3443.

[19] MUKHERJEE, K.G.; SATYANARAYANA, K.G.: Sturcture and properties of some vegetable fibres. Part 1: Sisal Fibre. *Journal of Materials Science* 19 (1984), P. 3925-3934.

[20] BRAZILIAN STANDARD NBR 11578. Cimento Portland Composto. Associação Brasileira de Normas Técnicas (ABNT), 1991 (In Portuguese).

[21] SILVA, F.A.; MOBASHER, B.; TOLEDO FILHO, R.D. Cracking mechanisms in durable sisal fiber reinforced cement composites. *Cement and Concrete Composites* (2009), IN PRESS.